2021

Impact of Mechanical Ventilation and Indoor Air Recirculation Rates on the Performance of an Active Membrane Energy Exchanger System

Andrew Fix
Department of Mechanical Engineering, Purdue University, United States of America,
fix.andrewj@gmail.com

James Braun

David Warsinger

Impact of Mechanical Ventilation and Indoor Air Recirculation Rates on the Performance of an Active Membrane Energy Exchanger System

Andrew FIX, James BRAUN, David WARSINGER*

School of Mechanical Engineering, Purdue University
West Lafayette, IN, United States of America
fixa@purdue.edu, jbraun@purdue.edu, dwarsing@purdue.edu

* Corresponding Author

ABSTRACT

As concern for indoor air quality grows, many buildings will likely opt to provide higher rates of outdoor air than would traditionally be specified. This imposes a challenge on air conditioning systems since the latent loads associated with ventilation air are much higher than those associated with recirculated air. Membrane-based technologies, which enable mechanical separation of water vapor from air, have recently emerged as promising candidates for efficiently providing dehumidification, however, limitations remain. To date, most modeling work on these types of systems has focused on 100% outdoor air configurations that employ isothermal dehumidification designs. However, we have proposed a design referred to as the Active Membrane Energy Exchanger (AMX) that integrates cooling and membrane dehumidification into one device (thus non-isothermal) for a range of benefits. This work presents a specific application of the AMX in a system configuration that includes the treatment of both outdoor ventilation air and recirculated air. The system's performance is analyzed over a broad range of ambient conditions and the effect of ventilation rates on the system performance is studied in detail. This configuration is found to be capable of providing three times the ventilation air of conventional systems with comparable or less energy consumption for the given conditions. Additionally, the optimal membrane module-outlet air temperature is found to be 18-20 ℃. Lastly, a case study using EnergyPlus building simulations shows that this configuration can reduce annual cooling energy requirements by as much as 34% in hot and humid cities for buildings with high latent loads and high ventilation rates.

1. INTRODUCTION

1.1 Background and Scope

Air conditioning and ventilation currently constitutes roughly 13% of the energy used in buildings in the United States, and buildings are the largest source of energy consumption by end-use sector (DOE, 2011). As temperatures gradually rise due to global warming, the energy consumption of heating, ventilation, and air conditioning (HVAC) will shift towards greater proportions of cooling (both sensible and latent) compared to current trends (Li *et al*., 2012). However, a concurrent problem that HVAC systems must tackle is that of indoor air quality. This issue has become readily apparent amid the COVID-19 pandemic, and HVAC associations across the globe have provided guidance on the topic. ASHRAE, REHVA, and SHASE all released strategies to help mitigate the spread of COVID-19, ranging from temperature and humidity settings to air cleaning equipment (Guo *et al.*, 2021). However, each organization agreed that windows should be opened, and outdoor air supply rates should be increased as much as possible. While this type of operation will improve indoor air quality, it will also introduce thermal challenges since conventional systems will suffer significant energy penalties associated with low-temperature condensation dehumidification.

Thus, there is a great need for alternative HVAC technologies for efficient treatment of outdoor air. Membrane based systems are an emerging technology for the separate treatment of sensible and latent cooling loads (Woods, 2014). However, two large gaps remain in the literature. First, existing modeling literature for membrane-based AC systems has focused on 100% outdoor air systems. This is quite limiting since most HVAC systems in commercial buildings employ both air recirculation and mechanical ventilation. Second, these membrane systems have been rigidly defined as isothermal processes and have not considered the potential benefits that could arise from an innovative combination of membrane dehumidification and sensible cooling into one process that still maintains decoupled sensible and latent effects. In this paper, we present a thermodynamic framework to study a novel configuration that combines membrane dehumidification and sensible cooling, termed the Active Membrane Energy Exchanger (AMX) (Fix *et al.*, 2021), in the context of a system with both ventilation and air recirculation.

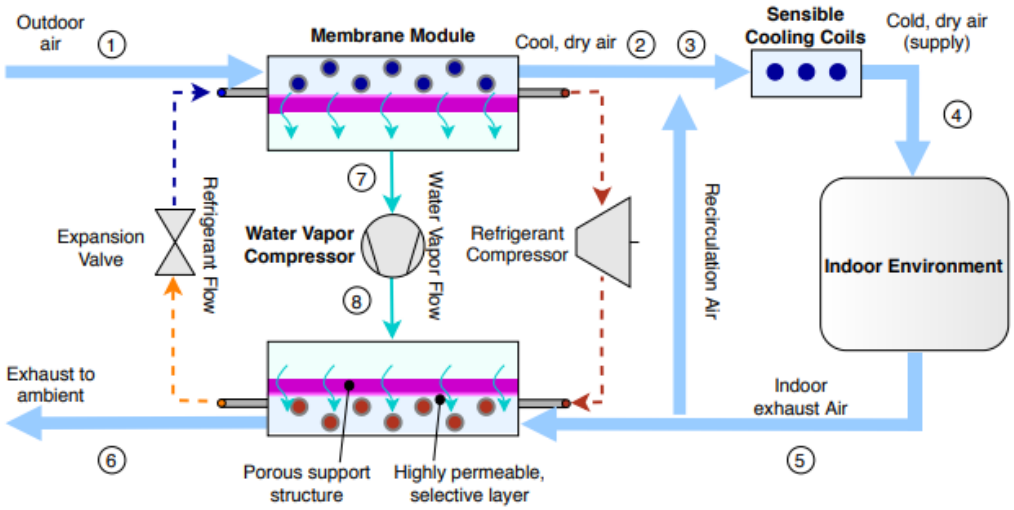

Figure 1: System schematic showing the novel Active Membrane Energy Exchanger device incorporated into a system with air recirculation and mechanical ventilation (AMX-R). The Active Membrane Energy Exchanger portion (two membrane modules and the integrated cooling cycle) provides all of the dehumidification required to meet the desired supply humidity and provides some sensible cooling. The mixed air is then sent to the separate sensible cooling coils.

1.2 Review of Membrane Dehumidification

The focus of this work is on active membrane dehumidification systems, which often employ a water vapor compressor (also referred to as a vacuum pump) to create a partial pressure gradient across the membrane to drive the dehumidification process. Many systems have been modeled, and some have been prototyped as well. The most basic embodiment of a membrane dehumidification device, in which the water vapor compressor operates directly between vacuum and atmospheric pressures, was prototyped, and it was found that the water vapor compressor is a very significant source of energy consumption (Bui *et al.*, 2017). Thus, many other configurations aim to minimize the pressure ratio across the compressor to reduce its power consumption. The use of a partial sweep stream on the vacuum permeate side of the membrane was used to reduce this pressure ratio, however there was a tradeoff between the sweep rate and dehumidification efficiency (Scovazzo and MacNeill, 2017). A theoretical low-pressure condensation strategy combined with membrane dehumidification was also investigated (Claridge *et al.*, 2019).

It has also been proposed to use two membrane modules, with a compressor operating between the two modules at small pressure ratios (Labban *et al.*, 2017). This approach relies on the vapor partial pressure difference across the membranes to cause dehumidification in the intake module and vapor rejection in the exhaust module. This approach shows great promise for high efficiency and broad applicability and served as the inspiration for the AMX design.

1.3 Review of Membrane Materials

While the thermodynamic framework presented in this work is developed such that it is independent from the membrane material properties, we provide a brief review of the materials and the characteristics that enable these types of technologies. The primary material properties that are emphasized are the permeance to water vapor and the selectivity to air. The permeance to water vapor describes the material's affinity to allow water vapor transport across the membrane, while the selectivity to air is the ratio of water vapor permeance to air permeance (thus describing the material's ability to block air transport). Generally, high permeance and high selectivity are desired.

Mixed-matrix membranes combine a continuous phase, often a polymer, with inorganic particles to modify/improve the material performance. Previously, the polymer Pebax 1657 was combined with graphene oxide to achieve both high permeance (~5,000 GPU) to water vapor and high selectivity to nitrogen (~80,000) (Akhtar *et al.*, 2017). Polyvinyl alcohol (PVA) has been combined with several hygroscopic materials, including triethylene glycol, to provide simple fabrication, high performance (~4,800 GPU) composite membranes, though the selectivity (~3,000) was not as high as some others (Bui *et al.*, 2017). Aside from mixed-matrix membranes, other thin-film materials have been explored. Freestanding graphene oxide membranes were prepared through a simple casting process, achieving a water vapor permeance of around 30,150 GPU and a selectivity of around 10,000 (Shin *et al.*, 2016).

2. SYSTEM DESCRIPTION

The focus of this work is on the system-level development and application of a thermodynamic framework to understand the performance of the novel AMX in a system that includes both air recirculation and mechanical ventilation, abbreviated AMX-R (Figure 1). Here, warm, humid outdoor air (1) enters the AMX portion of the system (Fig. 1, top left). The AMX dehumidifies the air through the use of selective membranes and a water vapor compressor. The AMX provides some sensible cooling to the air, but does not cool it all the way to the final supply temperature, as it is critical to avoid condensation (and its associated energy penalty). The dried, partially cooled air (2) is then mixed with the recirculated air (Fig. 1, top center). The AMX-R is modeled such that it dehumidifies the outdoor air to a low enough humidity content so that the mixed air stream will be at the desired supply humidity. Then, this mixed, dehumidified air (3) is sent to the separate cooling coils for the remaining sensible cooling required (Fig. 1, top right).

On the exhaust side (Fig.1 . bottom right), the exhaust air (5) that is not recirculated is sent to the exhaust membrane module (Fig. 1, bottom center). Here, the integrated condenser coils reject the heat absorbed by the module-integrated cooling coils. This heat rejection raises the temperature of the exhaust air and thus increases its capactity to hold water vapor. Simultaneously, the water vapor pulled out during dehumidification is slightly pressurized on the outlet side of the compressor, causing it to transport across the second membrane and flow into the exhaust air stream (Woods, 2014). This unique system design negates the need for an exhaust stream heat pump used in other designs (Labban *et al.*, 2017) and enables high cooling COP for part of the sensible load.

3. MODELING APPROACH

Engineering Equation Solver was used to develop system-level thermodynamic models for the AMX-R (Fig. 1) and for a baseline conventional system, modeled as a vapor compression system with recirculation and mechanical ventilation (VC-R) (Appendix, Figure A1). The models were developed using quasi-steady-state, open system mass and energy balances. Additionally, EnergyPlus building simulations were used to obtain reasonable building conditions (sensible and latent gain, indoor temperature, and ventilation rates) as well as for an annual energy performance case study. The vapor compression cycles were modeled separately, compared to commercial data, and integrated into the system-level models. The system-level modeling approach was validated in prior work by replicating modeling results for similar systems in the literature (Fix *et al.*, 2021).

3.1 Vapor Compression Cycle Models

A more detailed description of the vapor compression cycle models is presented by Fix et al. (2021). A simplified modeling approach was employed which relies on assumed heat exchanger subcooling, superheating, and pinch point temperature differences (Cengel and Boles, 2006). This is a common approach and allows the model to be generalized and thus easily used across a range of analyses. We assumed pinch point temperature differences for heat exchangers of 5 ℃, condenser refrigerant exit subcooling of 5ºC, and evaporator refrigerant exit superheating of 10 ºC (Barta *et al.*, 2020). Knowing these temperature differences, the desired supply temperature, the ambient temperature, and the temperature of the indoor exhaust stream, the model determines the thermodynamic states throughout the cycle.

The vapor compression cooling COP is calculated and fed into the system-level models. The modeled vapor compression cycle cooling COP's were compared against data for a commercial heat pump and found to match closely with an R^2 value of 0.992 (Fix *et al.*, 2021), enabling relatively accurate, system-level performance predictions.

3.2 Internal Load Energy Balance

The system-level models, both for the AMX-R and baseline VC-R, take several inputs, but the internal building sensible and latent loads are critical in defining the operation of the system. The AMX-R total mass flowrate is determined according to the internal sensible gain energy balance, shown in Equation 1;

$$\dot{Q}_s = \dot{m}_{air,total} c_{p,air} (T_5 - T_4) \quad (1)$$

Here, $\dot{Q}_s$ is the total sensible gain rate to the indoor air (due to internal sources (e.g., people, lights, computers), infiltration, and convection from interior surfaces (e.g., walls, ceilings, floors)), $c_{p,air}$ is the specific heat capacity of the indoor moist air, $\dot{m}_{air,total}$ is the dry air mass flowrate needed to meet the load, and T_4 and T_5 are the supply

temperature and indoor exhaust air temperature, respectively, as seen in Figure 1. T_4 is set to 13 ℃ throughout this work, and T_5 is assumed to be 24 ℃, except in the EnergyPlus case study in which T_5 is an input from the EnergyPlus results. In order to determine the quasi-steady-state indoor humidity, an energy balance is performed on the latent energy gain rate shown in Equation 2;

$$\dot{Q}_L = \dot{m}_{air,total} h_{fg,water} (\omega_5 - \omega_4) \tag{2}$$

Here, $\dot{Q}_L$ is the total latent gain rate for the indoor space (due to internal sources and infiltration) and $h_{fg,water}$ is the enthalpy of vaporization for water. ω_4 is the absolute humidity of the supply air stream, which is known (T_4=13 ℃, RH_4=90%). ω_5 is the absolute humidity of the indoor space/exhaust air stream and is solved for using Equation 2.

3.3 AMX Mass Transfer Balance

In order to define the dehumidification energy requirement, the desired humidity ratio at the outlet must be set accordingly. As previously mentioned, the AMX portion of the system dehumidifies the ventilation air to a low enough humidity such that the mixed air stream is at the desired supply humidity ratio. This implies that $\omega_3 = \omega_4$. Thus, a mass balance at the mixing point determines the required membrane module outlet humidity ratio, ω_2.

$$\dot{m}_v \omega_2 + \dot{m}_R \omega_5 = \dot{m}_{air,total} \omega_3 \tag{3}$$

Here, $\dot{m}_v$ is the dry air mass flowrate of outdoor ventilation air, $\dot{m}_R$ is the dry air mass flowrate of recirculated air, and ω_5 is the absolute humidity of the recirculated air, determined from the latent load energy balance. Knowing ω_2, the rate of water vapor removal from the incoming outdoor air stream is calculated according to Equation 4;

$$\dot{m}_{vapor} = \dot{m}_v (\omega_1 - \omega_2) \tag{4}$$

Similar to Equation 3, the absolute humidity at the outlet of the exhaust membrane module, ω_6, can be determined according to the mass balance shown in Equation 5;

$$\dot{m}_{vapor} + \dot{m}_v \omega_5 = \dot{m}_v \omega_6 \tag{5}$$

The outdoor air and indoor exhaust air temperatures, T_1 and T_5, are known, and the intake membrane module outlet air temperature, T_2, is assumed constant (discussion on this later). The exhaust membrane module outlet temperature, T_6, is solved for knowing the heat rejection rate from the integrated vapor compression cycle (Fix *et al.*, 2021). Thus, the water vapor partial pressure, P_{vapor}, is calculated at states 1, 2, 5, and 6. The average vapor partial pressure, $P_{vapor,avg}$, is then determined for both modules according to a logarithmic mean (Chen and Norford, 2020).

Lastly, the two water vapor vacuum pressures, P_7 and P_8, must be determined. We define the water vapor compressor operation by setting a constant pressure ratio across the compressor (Equation 6) and by assuming equal mass transport rates across each membrane module (Equation 7). Additionally, infinite selectivity is assumed given the high selectivity of many of the materials discussed, implying that only water vapor is present in the vacuum chambers.

$$PR = \frac{P_8}{P_7} \tag{6}$$

$$P_{vapor,avg,1-2} - P_7 = P_8 - P_{vapor,avg,5-6} \tag{7}$$

Each side of Equation 7 is derived from Fick's Law and assumes that each membrane module has the same membrane area and permeance to water vapor, thus these terms drop out from each side of the equation. Knowing the pressure across the water vapor compressor allows its power to be calculated with an assumed isentropic efficiency.

3.4 Baseline Comparison to a Conventional Vapor Compression System

The baseline vapor compression system with recirculation (VC-R) operates on very similar thermodynamic principles. However, in the conventional system (Figure A1), outdoor ventilation air is mixed directly with recirculation air before

entering the cooling coils. Here, the cooling coils are assumed to produce supply air at the same conditions as the final supply air in the AMX-R (13 ℃, 90% RH). However, in order to achieve the dehumidification, water is condensed out of the air by the cooling coils. The energy associated with both the sensible cooling and condensation dehumidification are accounted for in the power consumption calculations for the cooling coils in the VC-R system.

3.5 AMX-R System Performance Metrics

The primary performance metrics used in this work are the system COP and system energy savings. In order to determine these values, the cooling power requirements for each cooling cycle (both the membrane module integrated cycle and the separate/conventional cycle) are determined according to Equations 8;

$$\dot{W}_c = \frac{\dot{Q}_C}{COP_C} \tag{8}$$

$\dot{Q}_C$ is the heat removal rate from the air, provided either by the membrane module integrated cooling coils or the separate sensible cooling coils. In the AMX-R, $\dot{Q}_c$ only accounts for sensible cooling for both sets of cooling coils since the membrane handles the latent load. However, in the VC-R (baseline) system, $\dot{Q}_c$ accounts for both sensible and latent cooling. COP_c is the vapor compression cycle COP, for either the module integrated or separate cooling cycle, determined by the cycle models described in Section 3.1. $\dot{W}_c$ is determined for both cooling cycles using the respective values for $\dot{Q}_c$ and COP_c (subscript "MM" is for the integrated cycle, "SC" is for the separate cycle, and "B" is for the baseline VC-R system).

Since the mass flowrate of water vapor is known from Equation 4 and the vapor pressures are known from Equations 6 and 7, the enthalpy at states 7 and 8 can be used to calculate the water vapor compressor power consumption, $\dot{W}_{WVC}$, by assuming an isentropic efficiency. Lastly, the fan power consumption, $\dot{W}_{fan}$ is determined according to an assumed pressure rise found in typical rooftop units and assuming a fan efficiency of 30% (Fix *et al.*, 2021). The system COP for the AMX-R is defined based on the sensible and latent loads for the indoor air, as shown in Equation 9;

$$COP_{MHX-R} = \frac{\dot{Q}_L + \dot{Q}_S}{\dot{W}_{c,MM} + \dot{W}_{c,SC} + \dot{W}_{fan} + \dot{W}_{WVC}} \tag{9}$$

Similarly, the system COP for the baseline VC-R system is defined according to Equation 10;

$$COP_{VC-R} = \frac{\dot{Q}_L + \dot{Q}_S}{\dot{W}_{c,B} + +\dot{W}_{fan}} \tag{10}$$

Additionally, the energy savings are determined as the difference between the AMX-R and the VC-R total system power consumptions at any given test condition.

3.6 Annual Building Performance Simulations

EnergyPlus was used to provide a real-world case study on the performance of the AMX-R in various locations and building types, as well as to provide reasonable operating parameters for some of the parametric studies. Using the "Commercial Prototype Building Models" developed by Pacific Northwest National Laboratory, hourly reports were generated for various building types and locations including the following information:

- Outdoor Air Temperature, T_1
- Outdoor Absolute Humidity, ω_1
- Internal Sensible Gain Rate, $\dot{Q}_s$
- Internal Latent Gain Rate, $\dot{Q}_L$
- Internal Temperature, T_5
- Mechanical Ventilation Mass Flowrate, $\dot{m}_v$

With this annual hourly data, all non-cooling hours were filtered out. Cooling hours were defined as hours for which the outdoor air temperature was greater than 20 ℃ and the sensible load was negative (which implies required cooling in EnergyPlus). Then, these six variables were used as inputs in the EES models for the AMX-R and VC-R to determine the systems' COP's and power consumption for each cooling hour throughout a typical year.

4. RESULTS AND DISCUSSION

4.1 Overall AMX-R System COP

As previously mentioned, one of the primary performance metrics for this system is the COP. In order to provide a parametric analysis of the system COP, indoor cooling loads, temperatures, and ventilation rates must be set. As such, these previously mentioned values were taken from an EnergyPlus simulation for a "Medium Office" in Houston, Texas. The values used for the parametric study shown in Figure 2 are summarized in Table 1 and were taken from the EnergyPlus simulation at 2 PM on June 1 (a notably hot and humid hour).

Table 1: Typical Building Operation Parameters from EnergyPlus

Parameter	Symbol	Value
Indoor Space Sensible Gain Rate	$\dot{Q}_S$	114.3 kW
Indoor Space Latent Gain Rate	$\dot{Q}_L$	12.9 kW
Internal Temperature	T_5	24 ℃
Ventilation Mass Flowrate	$\dot{m}_V$	2.71 kg/s

In addition to these inputs, several other values must be set in order to evaluate the system performance. Table 2 summarizes the system-level assumptions. The water vapor compressor isentropic efficiency was chosen based on a review of similar system modeling publications as well as typical ranges for compressor efficiencies. A sensitivity analysis on this parameter is provided by Fix et al. (2021).

Table 2: System-Level Operation Assumptions

Parameter	Symbol	Value
Compressor Pressure Ratio	PR	3
Compressor Isentropic Efficiency	η	70%
Module Outlet Air Temperature	T_2	20 ℃
Supply Air Temperature	T_4	13 ℃
Supply Air Relative Humidity	RH_4	90%

Under these operating conditions, Figure 2 shows the AMX-R system COP over a range of outdoor air conditions.

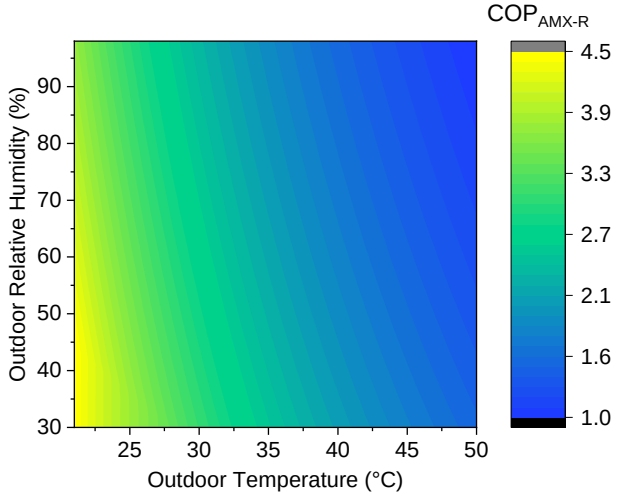

Figure 2: System COP of the AMX-R configuration as a function of the outdoor air temperature and humidity, presented for outdoor air conditions ranging between 20-50 ℃ and 30-100% relative humidity.

As might be expected, the system achieves higher COP's at lower ambient temperatures, where the vapor compression cooling cycle operates at a higher COP. The overall system COP deterioration at higher temperatures is more gradual

than that of the conventional system, leading to greater relative energy savings at more extreme conditions. Additionally, the COP is a weaker function of the relative humidity, evident in the gradual COP gradient in the y direction of Figure 2. For example, at a temperature of 31.6 ℃, which corresponds to the temperature for the given design hour from EnergyPlus (Table 1), the AMX-R experiences a system COP difference of approximately 28% moving from 30% relative humidity to 100%. For the same conditions, the VC-R system experiences a 57% difference in COP. This implies that, while greater humidity places additional power requirements on both systems, the energy penalties aren't as dramatic in the AMX-R as those found for the conventional system used herein.

4.2 Ventilation Air Temperature Optimization

One critical operating parameter in any air conditioning system is the supply air temperature. Since the AMX-R system provides some sensible cooling within the dehumidification stage to enable useful energy recovery and higher COP cooling for part of the load, the air temperature at the outlet of the AMX unit (T_2) can be optimized. Changing this outlet temperature effects the mixed air stream temperature, and thus the load imposed on the separate cooling coils, and it affects the COP of the integrated cooling coils. Thus, there is a non-obvious relation between the overall system performance and the membrane module outlet temperature (T_2). This relation is addressed in Figure 3.

As can be seen, the overall system COP is not very sensitive to the module outlet air temperature, with a maximum change of 1.3% over the given range. The optimal temperature where the COP is maximized occurs at around 18-20 ℃. Given the concurrent goal of this system to avoid condensation, setting T_2 to 20 ℃ (at the higher end of the optimal range) as the default is a sound choice. Additionally, a key feature of the AMX-R is the use of the waste heat from the integrated cooling cycle to prevent the exhaust air stream from becoming oversaturated when expelling the water vapor in the exhaust membrane module. So, the integrated cooling cycle needs to operate at sufficiently low temperatures to enable this waste heat use. T_2=20 ℃ meets this criterion for the analysis presented herein but could vary for different scenarios.

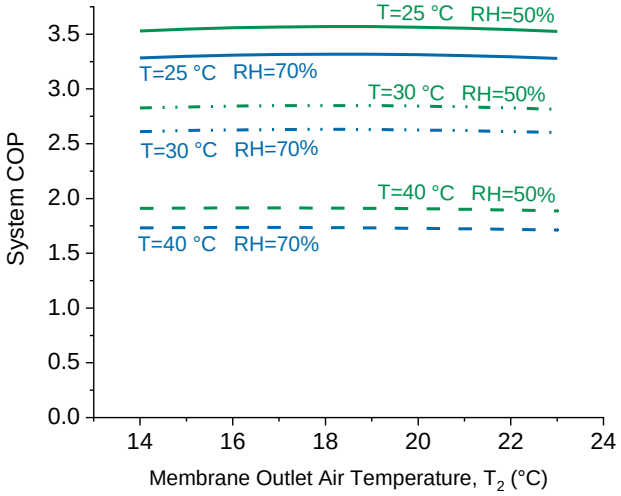

Figure 3: AMX-R system COP as a function of the membrane module outlet air temperature for several ambient temperature and humidity conditions. This figure shows the optimal range of module outlet air temperatures.

4.3 Effect of the Ventilation Rate

As was discussed in the introduction, increasing the ventilation, or outdoor air, rates in buildings is a commonly employed strategy for improving indoor air quality and mitigating virus spread. However, doing so imposes greater cooling loads on the air conditioning systems. Therefore, the AMX, which is more efficient at treating outdoor air, presents a unique opportunity to increase the ventilation rates beyond the current ASHRAE specifications while maintaining reasonably efficient air conditioning.

Figure 4 shows the power consumption of the AMX-R and the conventional VC-R as a function of the ventilation air ratio. This result was produced using the building data presented in Table 1 along with an outdoor temperature of 31.6 ℃ and an absolute humidity of 0.0156 (taken from the same EnergyPlus hour described in Table 1). For these conditions, a set mass flowrate of air is required to meet the load, so changing the relative amount of outdoor air being supplied changes the total power consumption. The AMX-R uses less power over the entire range, signifying that the AMX-R is the more efficient option for any ventilation rate. To further elucidate this behavior, the dotted lines show that the VC-R can only provide approximately 33% outdoor air before the power consumption of the VC-R exceeds that of the AMX-R operating at 100% outdoor air.

Figure 5 takes this analysis a step further by comparing the performance of the AMX-R at several ventilation rates against the VC-R operating at the baseline ventilation rate from Table 1 as a function of the outdoor air temperature

and at 50% relative humidity. The plot highlights the fact that the ventilation mass flowrate can be nearly tripled in the AMX-R while still maintaining a higher or comparable overall COP than the conventional VC-R system.

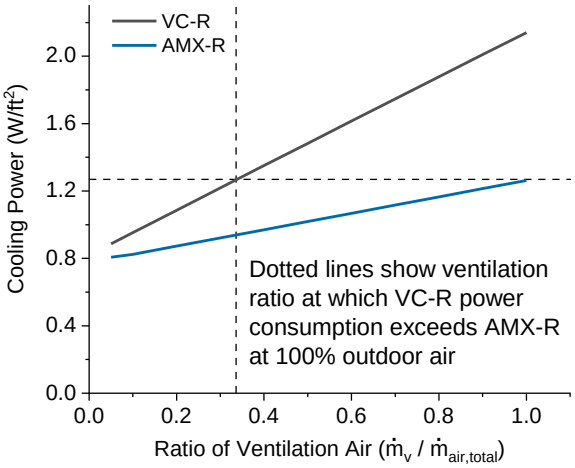

Figure 4: Cooling power consumption for the AMX-R and VC-R systems as a function of the ratio of the ventilation air to total air mass flowrates for the conditions specified in Table 1.

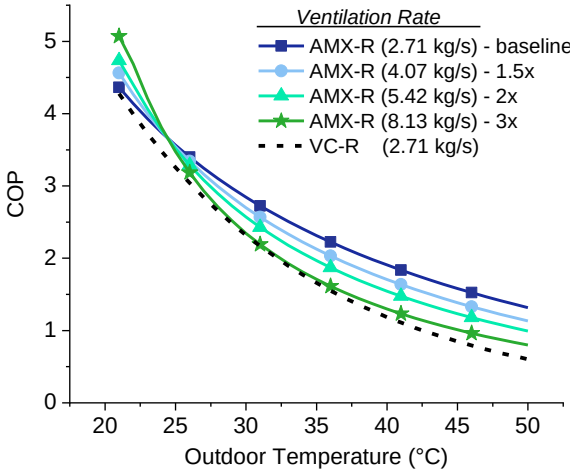

Figure 5: System COP of the AMX-R for various ventilation mass flowrates ($\dot{m}_v$) compared to the VC-R system operating at the baseline ventilation rate specified by ASHRAE 62.1 (from EnergyPlus).

4.4 EnergyPlus Case Study

Here, we provide a case study for several different locations and building types and compare the total cooling power consumption between the AMX-R and VC-R in each case. The "Prototype Commercial Building Models" developed by PNNL use the minimum ventilation rate specified by ASHRAE 62.1, and both systems (AMX-R and VC-R) used the same ventilation rates from EnergyPlus when determining the energy savings. Figure 6 presents the monthly cooling electricity savings, normalized by the building floor space, in kWh/ft² for a "Medium Office" prototype building simulated in five major US cities. The floor area for each building type is summarized in Table A1 in the Appendix. The energy savings peak in the mid-late summer months, which is a reasonable expectation in the US. Additionally, there is a large difference between the profiles for Houston, which is a notoriously hot and humid city, and Los Angeles, which is cooler and drier So, we expect to see greater energy savings in hot and humid climates.

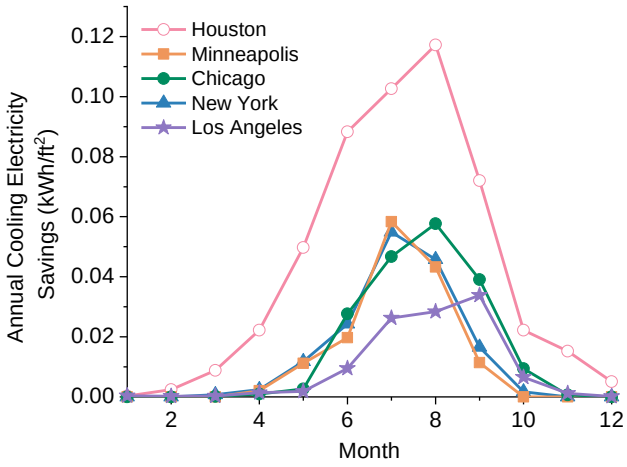

Figure 6: Normalized monthly cooling electricity savings profile for a "Medium Office Building" in five major US cities spanning numerous climate zones, generated using EnergyPlus building simulations.

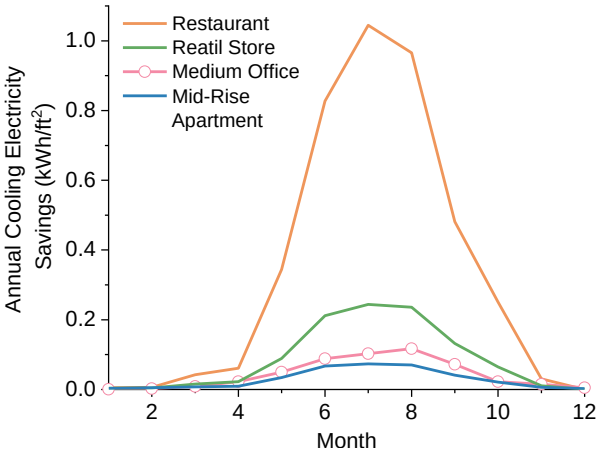

Figure 7: Normalized monthly cooling electricity savings profile for several different building types located in Houston, Texas, generated using EnergyPlus building simulations.

Given the higher savings in Houston, Figure 7 presents the normalized annual cooling electricity savings for four different building types (Restaurant, Retail Store, Medium Office, and Mid-Rise Apartment) simulated in Houston. What is noticeable here is the large savings for the restaurant. This stems from two sources: 1) the restaurant has significant internal sensible and latent loads and 2) the ventilation rate is relatively large and constant, representing a significant portion of power consumption considering the climate. Table 3 summarizes the annual savings.

Table 3: Summary of annual cooling electricity savings for the AMX-R from the EnergyPlus simulations

Location	Building Type	Annual Cooling Electricity Savings (kWh/ft^2-year)	Annual Cooling Electricity Savings (%)
Houston	Medium Office	0.527	23.3
Minneapolis	Medium Office	0.149	18.8
Chicago	Medium Office	0.192	18.4
New York	Medium Office	0.166	17.1
Los Angeles	Medium Office	0.115	18.3
Houston	Restaurant	4.20	32.2
Houston	Retail Store	1.07	33.7
Houston	Mid-Rise Apartment	0.352	19.4

5. CONCLUSIONS

In this work, we presented a steady-state thermodynamic framework to study the air conditioning energy efficiency potential of the Active Membrane Energy Exchanger (AMX) in a system that includes both mechanical ventilation and indoor air recirculation. The system was found to provide a very high efficiency alternative to conventional systems, motivating future analysis, experimental evaluation, and prototype development. The key conclusions are:

- The optimal temperature for the air leaving the intake membrane module is approximately 18-20 ℃, though the system performance is not very sensitive to this parameter.
- The AMX-R can provide nearly three times as much outdoor ventilation air with power consumption comparable to the baseline VC-R system providing the standard ventilation flowrate.
- The EnergyPlus case studies showed that the AMX can achieve annual cooling electricity savings as high as 4.2 kWh/ft^2 in hot and humid cities for buildings with high internal load densities and ventilation rates.
- The AMX is a useful design for the next generation of HVAC technologies which will seek to efficiently provide greater rates of outdoor air to improve indoor air quality.

NOMENCLATURE

COP	coefficient of performance	(-)
c_p	specific heat capacity	(kJ/kg-K)
GPU	gas permeance units	(-)
h	specific enthalpy	(kJ/kg)
$\dot{m}$	mass flowrate	(kg/s)
$P_{vapor,avg}$	average water vapor pressure	(kPa)
PR	pressure ratio	(-)
PVA	polyvinyl alcohol	(-)
$\dot{Q}$	heat transfer rate	(kW)
RH	relative humidity	(%)
T	temperature	(℃)
$\dot{W}$	power consumption	(kW)

ω	absolute humidity	(kg/kg)

Subscript

B	baseline (referring to the baseline VC-R system)
c	cooling
L	latent
MM	membrane module (relating to the integrated cooling cycle)
R	recirculation air
S	sensible
SC	separate cooling coils
v	ventilation (outdoor air)
vapor	water vapor
WVC	water vapor compressor

REFERENCES

Akhtar, F. H., Kumar, M., & Peinemann, K. V. (2017). Pebax®1657/Graphene oxide composite membranes for improved water vapor separation. *Journal of Membrane Science, 525*, 187–194.

Barta, R. B., Ziviani, D., & Groll, E. A. (2020). Experimental analyses of different control strategies of an R-410A split-system heat pump by employing a turbomachinery expansion recovery device. *International Journal of Refrigeration, 112*, 189–200.

Bui, D. T., Wong, Y., Thu, K., Oh, S. J., Kum Ja., M., Ng, K. C., Raisul, I., & Chua, K. J. (2017). Effect of hygroscopic materials on water vapor permeation and dehumidification performance of poly(vinyl alcohol) membranes. *Journal of Applied Polymer Science*, *134*, 44765.

Bui, D. T., Kum Ja, M., Gordon, J. M., Ng, K. C., & Chua, K. J. (2017). A thermodynamic perspective to study energy performance of vacuum-based membrane dehumidification. *Energy, 132*, 106–115.

Cengel, Y. & Boles, M. (2006). *Thermodynamics: An Engineering Approach.* New York: McGraw Hill.

Chen, T., & Norford, L. K. (2020). Energy performance of next-generation dedicated outdoor air cooling systems in low-energy building operations. *Energy and Buildings, 209*, 109677.

Claridge, D. E., Culp, C., Liu, W., Pate, M., Haberl, J., Bynum, J., Tanskyi, O., & Schaff, F. (2019). A new approach for drying moist air: The ideal Claridge-Culp-Liu dehumidification process with membrane separation, vacuum compression and sub-atmospheric condensation. *International Journal of Refrigeration, 101*, 211–217.

Fix, A., Braun, J., & Warsinger, D. (2021). International Patent Application. Application Number PCT/US21/19314.

Fix, A., Braun, J., & Warsinger, D. (2021). Vapor-selective Active Membrane Energy Exchanger for high efficiency outdoor air treatment. *Applied Energy, (in review).*

Guo, M., Xu, P., Xiao, T., He, R., Dai, M., & Miller, S. L. (2021). Review and comparison of HVAC operation guidelines in different countries during the COVID-19 pandemic. *Building and Environment, 187*, 107368.

Labban, O., Chen, T., Ghoniem, A. F., Lienhard, J. H., & Norford, L. K. (2017). Next-generation HVAC: Prospects for and limitations of desiccant and membrane-based dehumidification and cooling. *Applied Energy, 200*, 330–346.

Li, D. H. W., Yang, L., & Lam, J. C. (2012). Impact of climate change on energy use in the built environment in different climate zones - A review. *Energy, 42*, 103–112.

Lu, D. B., & Warsinger, D. M. (2020). Energy savings of retrofitting residential buildings with variable air volume systems across different climates. *Journal of Building Engineering*, 30, 101223.

Scovazzo, P., & MacNeill, R. (2019). Membrane module design, construction, and testing for vacuum sweep dehumidification (VSD): Part I, prototype, development and module design. *Journal of Membrane Science, 576*, 96–107.

Sekar, A., Fix, A., & Warsinger, D. (2021). Optimizing Combined Membrane Dehumidification with Heat Exchangers using CFD for High Efficiency HVAC Systems. *Journal of Membrane Science, (in review).*

Shin, Y., Liu, W., Schwenzer, B., Manandhar, S., Chase-Woods, D., Engelhard, M. H., Devanathan, R., Fifield, L. S., Bennett, W. D., Ginovska, B., & Gotthold, D. W. (2016). Graphene oxide membranes with high permeability and selectivity for dehumidification of air. *Carbon, 106*, 164–170.

U.S. Department of Energy. (2012). Buildings Energy Data Book. *Office of Energy Efficiency and Renewable Energy.*

Woods, J. (2014). Membrane processes for heating, ventilation, and air conditioning. *Renewable and Sustainable Energy Reviews, 33*, 290–304.

APPENDIX

The baseline system used throughout this work, the vapor compression system with air recirculation and mechanical ventilation (VC-R), is depicted below in Figure A1.

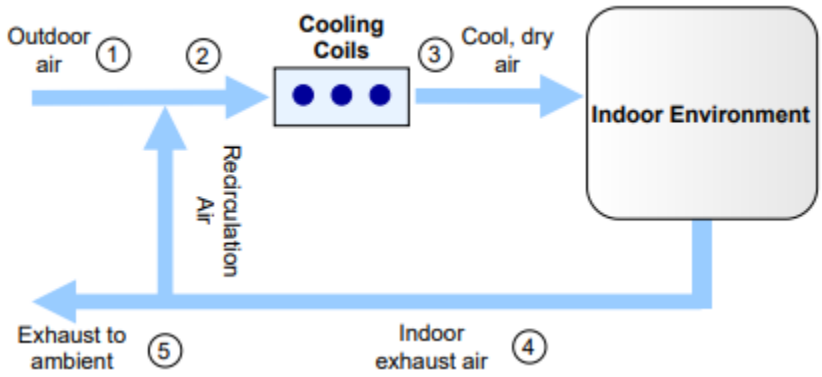

Figure A1: Conventional vapor compression system that features both air recirculation and mechanical ventilation (VC-R) used as the baseline system for comparison in this work.

The only sources of energy consumption in this system are for the fan used to move air through the system and the cooling coils. The conditions at state 2 are determined from the same mass balance and isenthalpic mixing analysis used for the mixing point in the AMX-R system. The cooling coils provide all of the sensible cooling and condensation dehumidification. The power required for both of these forms of cooling is accounted for by using the vapor compression cooling cycle COP determined by the cycle model discussed herein and presented by Fix et al. (2021).

Table A1: Summary of the building floor space for each of the EnergyPlus prototype commercial building models utilized in this work.

Building Type	**Floor Area (ft^2)**
Medium Office	53,600
Restaurant	5,502
Retail Store	24,695
Mid-Rise Apartment	33,700